

# Recurrent Neural Networks for Partially Observed Dynamical Systems

Uttam Bhat

*University of California, Santa Cruz, CA, 95064, United States\**

Stephan B. Munch

*Applied Mathematics, University of California, Santa Cruz, CA, 95064, United States†*

(Dated: September 27, 2021)

Complex nonlinear dynamics are ubiquitous in many fields. Moreover, we rarely have access to all of the relevant state variables governing the dynamics. Delay embedding allows us, in principle, to account for unobserved state variables. Here we provide an algebraic approach to delay embedding that permits explicit approximation of error. We also provide the asymptotic dependence of the first order approximation error on the system size. More importantly, this formulation of delay embedding can be directly implemented using a Recurrent Neural Network (RNN). This observation expands the interpretability of both delay embedding and RNN and facilitates principled incorporation of structure and other constraints into these approaches.

## I. INTRODUCTION

Forecasting dynamical systems is important in many disciplines. Weather and climate [1], ecology [2, 3], biology, [4, 5], fluid dynamics [6] etc. are generally modeled with nonlinear, discrete time equations or continuous time differential equations. In many cases, these non-linear systems are chaotic and subject to stochastic drivers. However, the empirical data available are often incomplete; It is common to observe only a subset of the state variables or measure some coarse-grained statistic of the underlying state. In such a situation, all hope is not lost; Takens embedding theorem [7] shows that time-delayed versions of a single observable can be used in place of the unobserved dimensions to reconstruct the attractor manifold permitting accurate short- and mid-term forecasts [8].

Takens theorem shows that any universal function approximator (given enough data) would be able to infer the function mapping the delay state vector to its future value. However, the proof of Takens' theorem is topological and non-constructive. Therefore, one approach to reconstruct dynamics using partial state variables is accomplished by using off-the-shelf function approximation methods to infer the function mapping the delay vector to its future values from time series data.

Due to the recent developments in machine learning, there are abundant choices for tools to perform nonlinear regression. The common candidates are local linear regressions, neural networks and Gaussian processes [9–13]. Recurrent Neural Networks (RNN) and its variants are some of the most widely used tools for time series prediction. Although RNNs have been successfully applied to forecasting in a wide range of problems, literature on the mathematical reasons why they work so well is largely lacking [14, 15]. Early justifications for using a recurrent

architecture include 1) being able to store temporal information [16], 2) neural networks with feedback capture time dependencies better, 3) are natural candidates for nonlinear autoregressive models [17], 4) leads to reduced number of parameters due to weight sharing [18]. RNNs were also used for time series prediction due to their ability to be continually trained [19]

Here we present a new approach to delay embedding through simple algebraic manipulation of the dynamical equations. We derive an approximation to the delay dynamics in terms of the original dynamics. We hypothesize that this approximation allows us to infer the delay map more efficiently with less data due to two reasons - 1) the original dynamics will be smoother than the nested compositions, and 2) the original dynamics are generally of smaller dimensionality than the delay function. We show how the prediction error in this framework may be approximated enabling comparisons across different modeling schemes and permits us to quantitatively evaluate the effects missing state variables. We simulate commonly used nonlinear dynamic systems to determine the efficacy of the approximation through examples

We use this approximation to encode a Recurrent Neural Network (RNN) to accomplish forecasting. Connections between dynamical system and RNN have been made in the past [20–22]. However, these connections do not take advantage of the recurrent nature of partially observed dynamics.

In the next section, we calculate the first order error due to partial observation of a system. We then develop a recursive approximation of the dynamics using only the observed states, and calculate the first-order expansion of the covariance of the recursion error. In section III, we develop a recurrent neural network architecture that uses the recursive structure of the dynamics of the observed states and demonstrate the improved performance in common biophysical systems. We use short simulated time-series as the effectiveness of the RNN structure over feed-forward networks is most evident when the number of training points is less than a hundred. Finally, we discuss the potential for using other function approximators

\* ubhat@ucsc.edu

† steve.munch@noaa.gov

to take advantage of the general structure of dynamics to achieve more efficient representations of data.

## II. RECURSIVE EXPANSION OF DYNAMICS

Assume the dynamics are completely represented with a system of  $M$  state variables, say  $\mathbf{z}_t = \{z_{1,t}, z_{2,t}, \dots, z_{M,t}\}^T$  and the dynamics are given by

$$\begin{aligned} \frac{dz_1}{dt} &= f_1(\mathbf{z}_t) \\ &\vdots \\ \frac{dz_M}{dt} &= f_M(\mathbf{z}_t) \end{aligned} \quad (1)$$

However, the subsequent arguments are more transparent in discrete time, so we work with the corresponding flow map integrated on a unit time step,  $z_{1,t} = F_1(\mathbf{z}_{t-1}), \dots, z_{M,t} = F_M(\mathbf{z}_{t-1})$  which we write compactly as  $\mathbf{z}_t = \mathbf{F}(\mathbf{z}_{t-1})$

Since our focus is on partially observed systems, we split the state variables  $\mathbf{z}_t$  into two subsets:  $\mathbf{x}_t = \{z_{1,t}, z_{2,t}, \dots, z_{n,t}\}^T$  representing the observed state variables and  $\mathbf{y}_t = \{z_{n+1,t}, \dots, z_{M,t}\}^T$  containing the remaining, unobserved state variables. We re-write the dynamics as

$$\begin{aligned} \mathbf{x}_t &= \mathbf{F}(\mathbf{x}_{t-1}, \mathbf{y}_{t-1}) \\ \mathbf{y}_t &= \mathbf{G}(\mathbf{x}_{t-1}, \mathbf{y}_{t-1}) \end{aligned} \quad (2)$$

where  $\mathbf{F}$  represents the maps for the  $n$  observed states and  $\mathbf{G}$  represents the maps for the  $M - n$  unobserved states.

There are several ways to proceed, including (i) implicitly accounting for the unobserved states using time lags ([23, 24]), or (ii) modeling the complete dynamics and imputing the unobserved states using a hidden Markov approach (e.g. [25]). However, (ii) requires that we have a reasonable model for the complete state dynamics and significant problems arise when the model is inaccurate. Since we assume the complete dynamics are unknown, we focus on (i).

As a first step to doing this, we shift the map for the unobserved states back by one time step and substitute this into the dynamics for the observed states.

$$\begin{aligned} \mathbf{x}_t &= \mathbf{F}(\mathbf{x}_{t-1}, \mathbf{y}_{t-1}) \\ &= \mathbf{F}(\mathbf{x}_{t-1}, \mathbf{G}[\mathbf{x}_{t-2}, \mathbf{y}_{t-2}]) \\ &= E_{\mathbf{y}_{t-2}} [\mathbf{F}(\mathbf{x}_{t-1}, \mathbf{G}[\mathbf{x}_{t-2}, \mathbf{y}_{t-2}]) | \mathbf{x}_{t-1}, \mathbf{x}_{t-2}] + \varepsilon_t \\ &\approx \mathbf{F}(\mathbf{x}_{t-1}, \mathbf{G}[\mathbf{x}_{t-2}, \bar{\mathbf{y}}^{t-2}]) + \varepsilon_t \end{aligned} \quad (3)$$

where  $\bar{\mathbf{y}}^{t-2} = E[\mathbf{y} | \mathbf{x}_{t-1}, \mathbf{x}_{t-2}]$  is the conditional expectation for  $\mathbf{y}$  given the current and previous observation for  $\mathbf{x}$ . The apparent process noise  $\varepsilon_t$  is given by

$\varepsilon_t = \mathbf{F}[\mathbf{x}_{t-1}, \mathbf{G}(\mathbf{x}_{t-2}, \mathbf{y}_{t-2})] - \mathbf{F}[\mathbf{x}_{t-1}, \mathbf{G}(\mathbf{x}_{t-2}, \bar{\mathbf{y}}^{t-2})]$ . The approximation in line 4 of eq. (3) assumes  $\mathbf{F}$  and  $\mathbf{G}$  are almost linear for simplicity.

We can continue along this path an arbitrary number of times, each iteration adding another lag of  $\mathbf{x}$  and pushing back the dependence on  $\mathbf{y}$ . Doing so  $d$  times we get,

$$\begin{aligned} \mathbf{x}_t &= \mathbf{F}(\mathbf{x}_{t-1}, \mathbf{G}[\mathbf{x}_{t-2}, \dots, \mathbf{G}[\mathbf{x}_{t-d}, \bar{\mathbf{y}}^{t-d}] \dots]) + \varepsilon_t \\ &= \tilde{\mathbf{F}}_d(\mathbf{x}_{t-1}, \dots, \mathbf{x}_{t-d}) + \varepsilon_t \end{aligned} \quad (4)$$

where, in keeping with the previous notation,  $\bar{\mathbf{y}}^{t-d} = E[\mathbf{y}_{t-d} | \mathbf{x}_{t-1}, \dots, \mathbf{x}_{t-d}]$  and  $\varepsilon_t = \mathbf{F}(\mathbf{x}_{t-1}, \mathbf{G}[\mathbf{x}_{t-2}, \dots, \mathbf{G}[\mathbf{x}_{t-d}, \mathbf{y}_{t-d}] \dots]) - \mathbf{F}(\mathbf{x}_{t-1}, \mathbf{G}[\mathbf{x}_{t-2}, \dots, \mathbf{G}[\mathbf{x}_{t-d}, \bar{\mathbf{y}}^{t-d}] \dots])$ .

To estimate  $\varepsilon$ , we simulate the exact dynamics for 30000 time steps with sampling intervals matching the data generated in the next section. We discard the first 10000 points to remove transients. We use the next 10000 points to fit  $\bar{\mathbf{y}}^{t-d} = E[\mathbf{y}_{t-d} | \mathbf{x}_{t-1}, \dots, \mathbf{x}_{t-d}]$ . We calculate the recursion error,

$$\varepsilon_t = \mathbf{x}_t - \mathbf{F}(\mathbf{x}_{t-1}, \mathbf{G}[\mathbf{x}_{t-2}, \dots, \mathbf{G}[\mathbf{x}_{t-d}, \bar{\mathbf{y}}^{t-d}] \dots]) \quad (6)$$

as well as the first order approximation given by eq. (7). We calculate the RMS averages of both across  $t$ .

We can also use a first order approximation to estimate the covariance,  $\Sigma_t$  of the apparent process noise  $\varepsilon_t$ ,

$$\Sigma_t \approx \mathbf{P}_{t-1} \mathbf{Q}_{t-2} \dots \mathbf{Q}_{t-d} \mathbf{C}_{t-d} \mathbf{Q}_{t-d}^T \dots \mathbf{Q}_{t-2}^T \mathbf{P}_{t-1}^T \quad (7)$$

where  $\mathbf{P}_{t-1}$  is the matrix of partial derivatives of  $\mathbf{F}$  with respect to  $\mathbf{y}$  evaluated at  $\mathbf{x}_{t-1}$  and  $\bar{\mathbf{y}}^{t-1}$ ,  $\mathbf{Q}_{t-n}$  is the matrix of partial derivatives of  $\mathbf{G}$  with respect to  $\mathbf{y}$  evaluated at  $\mathbf{x}_{t-n}$  and  $E[\mathbf{y}_{t-n} | \mathbf{x}_{t-1}, \dots, \mathbf{x}_{t-d}]$ , and  $\mathbf{C}_{t-d}$  is the covariance matrix for  $\mathbf{y}_{t-d}$  conditional on  $\mathbf{x}_{t-1}, \dots, \mathbf{x}_{t-d}$ , i.e.  $\mathbf{C}_{t-d} = E[(\mathbf{y} - \bar{\mathbf{y}}^{t-d})(\mathbf{y} - \bar{\mathbf{y}}^{t-d})^T | \mathbf{x}_{t-1}, \dots, \mathbf{x}_{t-d}]$ .

Similar to the numerical estimation of the recursion error above, we can evaluate the first order approximation numerically from time series data by fitting  $\mathbf{C}_{t-d} = E[(\mathbf{y} - \bar{\mathbf{y}}^{t-d})(\mathbf{y} - \bar{\mathbf{y}}^{t-d})^T | \mathbf{x}_{t-1}, \dots, \mathbf{x}_{t-d}]$  from time series data. The first order approximation is accurate only for maps that are almost linear. For continuous time nonlinear dynamics, this would correspond to short sampling intervals.

Note that neither of these should be treated as strict bounds on practical accuracy. However, these can provide a baseline for the expected performance independent of the specifics of the forecast model.

## III. RECURRENT NEURAL NETWORK

In a practical setting, the dynamics given by eq. (2) can be learned from time-series data using delay vectors by fitting the function,

$$\mathbf{x}_t = \hat{\mathbf{F}}(\mathbf{x}_{t-1}, \dots, \mathbf{x}_{t-d}) \quad (8)$$

This can be implemented directly using standard machine learning methods [16, 26]. We implement a feedforward neural network to approximate  $\hat{\mathbf{F}}$  as a benchmark. The recursive form of eq. (4) suggests that the function approximator should be restricted among the space of functions that can be written as a recursive composition of lower dimensional functions  $\mathbf{F}$  and  $\mathbf{G}$ . This can be achieved by constructing a Recurrent Neural Network (RNN) that imitates the recursive form in eq. (4),

$$\begin{aligned}\hat{\mathbf{x}}_t &= \mathbf{W}_x \mathbf{f}_t + \mathbf{b}_x \\ \mathbf{f}_t &= \mathbf{a}_f (\mathbf{W}_f (\mathbf{x}_{t-1} \oplus \hat{\mathbf{y}}_{t-1}) + \mathbf{b}_f) \\ \hat{\mathbf{y}}_{t-1} &= \mathbf{W}_y \mathbf{g}_{t-1} + \mathbf{b}_y \\ \mathbf{g}_{t-1} &= \mathbf{a}_g (\mathbf{W}_g (\mathbf{x}_{t-2} \oplus \hat{\mathbf{y}}_{t-2}) + \mathbf{b}_g) \\ &\vdots \\ \hat{\mathbf{y}}_{t-d+1} &= \mathbf{W}_y \mathbf{g}_{t-d+1} + \mathbf{b}_y \\ \mathbf{g}_{t-d+1} &= \mathbf{a}_g (\mathbf{W}_g (\mathbf{x}_{t-d} \oplus \hat{\mathbf{y}}_{t-d}) + \mathbf{b}_g)\end{aligned}\quad (9)$$

Where the functions  $\mathbf{F}$  and  $\mathbf{G}$  are approximated as single layer neural networks with hidden layer  $\mathbf{f}$  and  $\mathbf{g}$ .  $\mathbf{a}_f$  and  $\mathbf{a}_g$  are the non-linear activation functions. In this study,  $\mathbf{a}_f = \mathbf{a}_g = \tanh$ . As  $\hat{\mathbf{y}}_t$  is just a linear function of  $\mathbf{g}_t$ , it can be absorbed into the parameters  $\mathbf{W}_f$ ,  $\mathbf{b}_f$ ,  $\mathbf{W}_g$ , and  $\mathbf{b}_g$  to obtain a simpler neural network,

$$\begin{aligned}\hat{\mathbf{x}}_t &= \mathbf{W}_x \mathbf{f}_t + \mathbf{b}_x \\ \mathbf{f}_t &= \mathbf{a}_f (\mathbf{W}_f (\mathbf{x}_{t-1} \oplus \mathbf{g}_{t-1}) + \mathbf{b}_f) \\ \mathbf{g}_{t-1} &= \mathbf{a}_g (\mathbf{W}_g (\mathbf{x}_{t-2} \oplus \mathbf{g}_{t-2}) + \mathbf{b}_g) \\ &\vdots \\ \mathbf{g}_{t-d+1} &= \mathbf{a}_g (\mathbf{W}_g (\mathbf{x}_{t-d} \oplus \mathbf{g}_{t-d}) + \mathbf{b}_g)\end{aligned}\quad (10)$$

The model parameters,  $\mathbf{W}_\alpha$  and  $\mathbf{b}_\alpha$  are chosen to minimize the loss function,

$$L = \sum_t \|\hat{\mathbf{x}}_t - \mathbf{x}_t^{(\text{data})}\|^2 \quad (11)$$

We train the parameters using backpropagation with RMSprop optimizer [27], and use early stopping [28] to avoid over-fitting the training data. Note, since this is a proof-of-concept demonstration, we did not regularize using a penalty term in the loss function, as this would make it difficult to explicitly compare the FNN and RNN in terms of the NN complexity. In the following sections, we use simulated time series from popular nonlinear dynamics models namely, 1) Lorenz 63 model [29] (3D), 2) the Duffing oscillator [30] (4D), and 3) the Lorenz 96 model [31] (5D). We train the RNN using training time-series of length 30 and 50 data points. We specifically focus on small training datasets as the advantage of the RNN over an FNN is larger in the data-poor regime. We divide the training data further into ‘train’ and ‘validation’ sets that contain 75% and 25% of the data respectively. The hidden layer sizes (dimensions of  $\mathbf{f}$  and  $\mathbf{g}$ ), as well as the early stopping parameter are chosen to

minimize validation loss. The errors reported are measured on out-of-sample ‘test’ data of the same size as the training datasets. The errors were averaged across 100 different realizations of the model in each case.

### A. Lorenz 63 model

Lorenz 63 is one of the most popular chaotic models. It is a first order differential equation modeling a simplified version of atmospheric convection [29].

$$\begin{aligned}\dot{x} &= \sigma(y - x) \\ \dot{y} &= x(\rho - z) - y \\ \dot{z} &= xy - \beta z\end{aligned}\quad (12)$$

We chose a sampling rate of 10 Hz so that the prediction problem was sufficiently non-trivial, but not impossible (see Table I for details). The observed variable is  $x$ . We compute training and validation loss for the neural networks with 2-20 hidden neurons (same number of hidden neurons for both  $\mathbf{f}$  and  $\mathbf{g}$  in case of RNN), and choose the one with the minimum validation loss. We also use the validation loss for ‘early stopping’ the training.

The optimal number of delays for both the FNN and the RNN is three (see Fig. 1). The optimal RMSE is statistically indistinguishable between the FNN and the RNN. However, the RNN has a robust performance across all number of delays (especially for the smaller dataset), which may be desirable for automated applications.

### B. Duffing oscillator

The Duffing oscillator is a second order differential equation with periodic forcing,

$$\ddot{x} + \delta \dot{x} + \beta x + \alpha x^3 = \gamma \cos(\omega t) \quad (13)$$

This can be re-written as a first-order autonomous system by introducing the variables  $y = \dot{x}$ ,  $v = \cos(\omega t)$  and  $z = \sin(\omega t)$ ,

$$\begin{aligned}\dot{x} &= y \\ \dot{y} &= \gamma v - \delta y - \beta x - \alpha x^3 \\ \dot{v} &= -\omega z \\ \dot{z} &= \omega v\end{aligned}\quad (14)$$

We chose a sampling rate of 1 Hz, as this model has a Lyapunov horizon that is roughly an order of magnitude larger than the Lorenz63 model (see Table I). The observed variable is  $x$ . The optimal number of delays in this case is four. The results for this model are qualitatively similar to the Lorenz 63 model, that is, at optimal number of delays, the performance is indistinguishable for the two neural networks, but RNN is more robust across the number of delays.

| Model              | parameters                            | Lyapunov exponent | Autocorrelation at $dt^a$ | RMSE ‘previous-value’ predictor <sup>b</sup> |
|--------------------|---------------------------------------|-------------------|---------------------------|--|
| Duffing Oscillator | [1., -1., 0.3, 0.5, 1.2]              | 0.166             | 0.667                     | 0.816  |
| Lorenz63           | $\rho = 28, \sigma = 10, \beta = 8/3$ | 0.905             | 0.869                     | 0.512  |
| Lorenz96           | $N = 5, F = 8$                        | $0.472 \pm 0.002$ | 0.866                     | 0.518  |

TABLE I. Descriptions of the datasets. a. Autocorrelation at the time-step used for predictions of the observed variable b. Normalized RMSE values from predicting using the previous value. Normalized such that using mean of the time-series leads to an RMSE= 1.

### C. Lorenz 96 model

Lorenz 96 is a popular model to test tools for chaotic time series prediction in a high dimensional setting [32, 33]. We generated time series data using the Lorenz 96 model [31]

$$\frac{dx_i}{dt} = (x_{i+1} - x_{i-2})x_{i-1} - x_i + F, \quad 1 \leq i \leq N \quad (15)$$

with parameters  $N = 5, F = 8$ . The dynamics are chaotic with Lyapunov exponent =  $0.472 \pm 0.002$ . Sampling rate is 10 Hz. The observed variable is  $x_1$ . The optimal number of delays is six.

The RNN shows significantly better performance as measured by the average RMSE in the case of the smaller dataset. There is also a significant difference between the optimal number of hidden neurons between the two NNs, with the RNN opting for lower number of hidden neurons indicating that the function to be fit is of a lower complexity.

## IV. DISCUSSION

In this study, we showed that choosing the neural network architecture that is derived from the structure of generating dynamics can lead to more efficient recovery of the dynamics from data. This is demonstrated by a significantly better prediction performance by the Recurrent Neural Network as compared to the Feedforward Neural Network in the small-data regime. We also see that the optimal number of hidden neurons is less for the RNN as compared to the FNN suggesting that the  $\mathbf{F}$  and  $\mathbf{G}$  functions are smoother than the function on the delay vector  $\tilde{\mathbf{F}}$ .

Our methods can be extended to take advantage of the structure of spatial dynamics as well. Since we expect

the spatial interaction structure to be sparse, we expect  $\mathbf{F}$  and  $\mathbf{G}$  to have a much lower dimensionality compared to fitting the full delay-embedding function.

Having dynamically meaningful units within the neural networks makes incorporating auxiliary information straightforward. For example, information about interactions between states can be implemented by conditioning the model to constrain the partial derivatives  $\partial H_i / \partial z_j = 0$  (where  $H \in \{F, G\}$  and  $z \in \{x, y\}$ ) that correspond to non-interacting states. This can be achieved through regularization or constraint optimization of neural networks.

In the field of statistical mechanics, the problem of unobserved states has been addressed by the Mori Zwanzig formulation where the Zwanzig operator is used to project the dynamics onto the linear subspace of the observed dynamics, where the ignored degrees of freedom appear as a memory term and a noise term. Calculating the memory term for nonlinear dynamics is non-trivial, and requires the expansion of the basis to lift the dynamics to a linear space. This can lead to an unbounded expansion of the state space in chaotic systems. In contrast, our approximation provides a straightforward way to incorporate the induced memory from partial observations.

In summary, we address the gap in the theoretical literature on the efficacy of recurrent neural networks. We show how partially observed dynamics can be restructured to reveal a recurrent structure, which can be learnt by fitting recurrent neural networks on time series data. We also provide a connection to time-delay embedding and discuss the potential applications of this methodology.

This work was supported by NOAA’s HPCC incubator.

- 
- [1] T. N. Palmer, A nonlinear dynamical perspective on model error: A proposal for non-local stochastic-dynamic parametrization in weather and climate prediction models, *Quarterly Journal of the Royal Meteorological Society* **127**, 279 (2001).
- [2] S. Lek, M. Delacoste, P. Baran, I. Dimopoulos, J. Lauga, and S. Aulagnier, Application of neural networks to modelling nonlinear relationships in ecology, *Ecological Modelling* **90**, 39 (1996).
- [3] Y. Luo, K. Ogle, C. Tucker, S. Fei, C. Gao, S. LaDeau, J. S. Clark, and D. S. Schimel, Ecological forecasting and data assimilation in a data-rich era, *Ecological Applications* **21**, 1429 (2011).
- [4] M. Lachowicz, Individually-based markov processes modeling nonlinear systems in mathematical biology, *Nonlinear Analysis: Real World Applications* **12**, 2396 (2011).

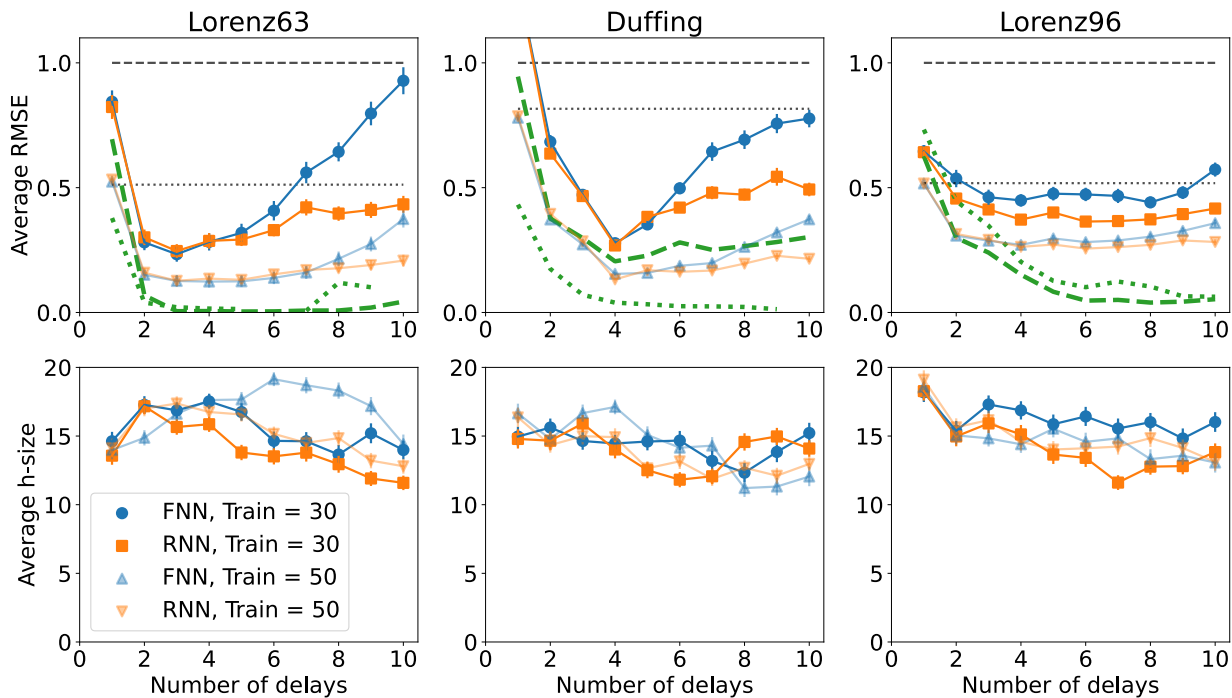


FIG. 1. (Top) Normalized RMSE as a function of number of delays from a FNN (blue) vs RNN (orange) for the Lorenz 63 model (left), Duffing (middle), and Lorenz 96 model in 5D (right) with parameters in Table I. The black dashed (dotted) lines are benchmark predictions using the time series mean (previous value). The green dashed (dotted) lines are numerical evaluations of the recursion error (4) (and its first-order approximation (7)). (Bottom) The average number of optimal hidden-neurons. Dark (light) colors are results for with a training size of 30 (50) data points

- [5] S. Imoto, S. Kim, T. Goto, S. Aburatani, K. Tashiro, S. Kuhara, and S. Miyano, Bayesian network and non-parametric heteroscedastic regression for nonlinear modeling of genetic network, *Journal of bioinformatics and computational biology* **1**, 231 (2003).
- [6] J. D. Farmer and J. J. Sidorowich, Predicting chaotic time series, *Physical review letters* **59**, 845 (1987).
- [7] F. Takens, Detecting strange attractors in turbulence, in *Dynamical systems and turbulence, Warwick 1980* (Springer, 1981) pp. 366–381.
- [8] G. Sugihara and R. M. May, Nonlinear forecasting as a way of distinguishing chaos from measurement error in time series, *Nature* **344**, 734 (1990).
- [9] M. Ragwitz and H. Kantz, Markov models from data by simple nonlinear time series predictors in delay embedding spaces, *Physical Review E* **65**, 056201 (2002).
- [10] S. P. Garcia and J. S. Almeida, Multivariate phase space reconstruction by nearest neighbor embedding with different time delays, *Physical Review E* **72**, 027205 (2005).
- [11] T. Qin, K. Wu, and D. Xiu, Data driven governing equations approximation using deep neural networks, *Journal of Computational Physics* **395**, 620 (2019).
- [12] M. Raissi, P. Perdikaris, and G. E. Karniadakis, Multi-step neural networks for data-driven discovery of nonlinear dynamical systems, arXiv preprint arXiv:1801.01236 (2018).
- [13] B. Lusch, J. N. Kutz, and S. L. Brunton, Deep learning for universal linear embeddings of nonlinear dynamics, *Nature communications* **9**, 1 (2018).
- [14] E. Weinan, C. Ma, S. Wojtowytsch, and L. Wu, Towards a mathematical understanding of neural network-based machine learning: What we know and what we don’t, arXiv preprint arXiv:2009.10713 (2020).
- [15] A. L. Caterini and D. E. Chang, *Deep Neural Networks in a Mathematical Framework* (Springer, 2018).
- [16] D. Mandic and J. Chambers, *Recurrent neural networks for prediction: learning algorithms, architectures and stability* (Wiley, 2001).
- [17] J. Connor, R. Martin, and L. Atlas, Recurrent neural networks and robust time series prediction, *IEEE Transactions on Neural Networks* **5**, 240 (1994).
- [18] I. Goodfellow, Y. Bengio, and A. Courville, *Deep learning* (MIT press, 2016).
- [19] R. J. Williams and D. Zipser, A Learning Algorithm for Continually Running Fully Recurrent Neural Networks, *Neural Computation* **1**, 270 (1989), <https://direct.mit.edu/neco/article-pdf/1/2/270/811849/neco.1989.1.2.270.pdf>.
- [20] J. L. Elman, Finding structure in time, *Cognitive science* **14**, 179 (1990).
- [21] M. Han, Z. Shi, and W. Wang, Modeling dynamic system by recurrent neural network with state variables, in *International Symposium on Neural Networks* (Springer, 2004) pp. 200–205.
- [22] H. Zimmermann and R. Neuneier, Modeling dynamical systems by recurrent neural networks, *WIT Transactions on Information and Communication Technologies* **25** (2000).
- [23] E. R. Deyle, M. Fogarty, C.-h. Hsieh, L. Kaufman, A. D. MacCall, S. B. Munch, C. T. Perretti, H. Ye, and G. Sugihara, Predicting climate effects on Pacific sardine, *Proceedings of the National Academy of Sciences* **110**, 6430

- (2013).
- [24] S. B. Munch, A. Giron-Nava, and G. Sugihara, Nonlinear dynamics and noise in fisheries recruitment: A global meta-analysis, *Fish and Fisheries* **19**, 964 (2018).
- [25] J. M. Morales, D. T. Haydon, J. Frair, K. E. Holsinger, and J. M. Fryxell, Extracting more out of relocation data: Building movement models as mixtures of random walks, *Ecology* 10.1890/03-0269 (2004).
- [26] S. B. Munch, V. Poynor, and J. L. Arriaza, Circumventing structural uncertainty: A bayesian perspective on nonlinear forecasting for ecology, *Ecological Complexity* **32**, 134 (2017), uncertainty in Ecology.
- [27] G. Hinton, N. Srivastava, and K. Swersky, Neural networks for machine learning lecture 6a overview of mini-batch gradient descent, Unpublished lecture **14** (2012).
- [28] L. Prechelt, Automatic early stopping using cross validation: quantifying the criteria, *Neural Networks* **11**, 761 (1998).
- [29] E. N. Lorenz, Deterministic nonperiodic flow, *Journal of atmospheric sciences* **20**, 130 (1963).
- [30] G. Duffing, *Erzwungene Schwingungen bei veränderlicher Eigenfrequenz und ihre technische Bedeutung*, 41-42 (Vieweg, 1918).
- [31] E. N. Lorenz, Predictability: A problem partly solved, in *Proc. Seminar on predictability*, Vol. 1 (1996).
- [32] A. Chattopadhyay, P. Hassanzadeh, and D. Subramanian, Data-driven predictions of a multiscale lorenz 96 chaotic system using machine-learning methods: reservoir computing, artificial neural network, and long short-term memory network, *Nonlinear Processes in Geophysics* **27**, 373 (2020).
- [33] P. D. Dueben and P. Bauer, Challenges and design choices for global weather and climate models based on machine learning, *Geoscientific Model Development* **11**, 3999 (2018).